The DeepMIP-Eocene model database and interactive web application versions 1.0

Sebastian Steinig[1,*], Ayako Abe-Ouchi[2], Agatha M. de Boer[3], Wing-Le Chan[2], Yannick Donnadieu[4], David K. Hutchinson[3,5], Gregor Knorr[6], Jean-Baptiste Ladant[7], Polina Morozova[8], Igor Niezgodzki[6,9], Christopher J. Poulsen[10], Evgeny M. Volodin[11], Zhongshi Zhang[12,13], Jiang Zhu[14], David Evans[15], Gordon N. Inglis[15], A. Nele Meckler[16], and Daniel J. Lunt[1]

[1]School of Geographical Sciences, University of Bristol, UK
[2]Atmosphere and Ocean Research Institute, University of Tokyo, Kashiwa, Japan
[3]Department of Geological Sciences, Stockholm University, Sweden
[4]Aix Marseille Univ, CNRS, IRD, INRA, Coll France, CEREGE, Aix-en-Provence, France
[5]Climate Change Research Centre, University of New South Wales Sydney, Sydney, Australia
[6]Alfred Wegener Institute, Helmholtz Centre for Polar and Marine Research, Bremerhaven, Germany
[7]Laboratoire des Sciences du Climat et de l'Environnement, LSCE/IPSL, CEA-CNRS-UVSQ, Université Paris-Saclay, Gif-sur-Yvette, France
[8]Institute of Geography, Russian Academy of Sciences, Moscow, Russia
[9]ING PAN - Institute of Geological Sciences Polish Academy of Sciences, Research Center in Kraków, Biogeosystem Modelling Group, Kraków, Poland
[10]Department of Earth Sciences, University of Oregon, Eugene, Oregon, USA
[11]Institute of Numerical Mathematics, Russian Academy of Sciences, Moscow, Russia
[12]NORCE Norwegian Research Centre, Bjerknes Centre for Climate Research, Norway
[13]Department of Atmospheric Science, School of Environmental Studies, China University of Geosciences, Wuhan, China
[14]Climate & Global Dynamics Laboratory, National Center for Atmospheric Research, USA
[15]School of Ocean and Earth Science, University of Southampton, UK
[16]Bjerknes Centre for Climate Research and Department of Earth Science, University of Bergen, Norway
[*]corresponding author: Sebastian Steinig (sebastian.steinig@bristol.ac.uk)

ABSTRACT

Paleoclimate model simulations provide reference data to help interpret the geological record and offer a unique opportunity to evaluate the performance of current models under diverse boundary conditions. Here, we present a database of 35 climate model simulations of the warm early Eocene Climatic Optimum (EECO; $\sim$ 50 million years ago) and corresponding preindustrial reference experiments. To streamline the use of the data, we apply standardised naming conventions and quality checks across eight modelling groups that have carried out coordinated simulations as part of the Deep-Time Model Intercomparison Project (DeepMIP). Gridded model fields can be downloaded from an online repository or accessed through a new web application that provides interactive data exploration. Local model data can be extracted in CSV format or visualised online for streamlined model-data comparisons. Additionally, processing and visualisation code templates may serve as a starting point for advanced analysis. The database and online platform aim to simplify accessing and handling complex data, prevent common processing issues, and facilitate the sharing of climate model data across disciplines.

Background & Summary

Past climate changes provide an opportunity to better understand how key components of the climate system might change under anthropogenic greenhouse gas emissions and thus help constrain future climate change[1]. Comparisons with paleoclimate data allow us to evaluate climate models under atmospheric CO_2 scenarios similar to those possible in the near future. Furthermore,

these paleoclimate model simulations provide global, physically consistent reference data to support the interpretation of paleoclimatic data across a wide range of disciplines, e.g. in geology, biology, and geochemistry.

One of the most well-studied past time intervals with respect to model-data comparison is the early Eocene Climatic Optimum (EECO; ~53.3 to 49.1 million years ago[2]) as it provides an analogue for future very high emission scenarios[3]. It was characterised by atmospheric CO_2 concentrations of ~1,500 ppm[4] and global mean surface temperatures (GMSTs) 10 to 16 °C warmer than pre-industrial[5]. Several modelling studies have focused on improving our understanding of the mechanisms and implications of EECO warmth[6–10] and ultimately motivated the formulation of the Eocene Modelling Intercomparison Project (EoMIP)[11]. While limited due to its opportunistic design, EoMIP nonetheless highlighted the possibility of using multi-model ensembles to systematically assess model-model and model-data differences in our understanding of Eocene climate.

Building on this potential, DeepMIP – the Deep-Time Model Intercomparison Project – was designed to provide a consistent framework to carry out coordinated EECO model experiments[12]. Eight modelling groups performed a total of 35 model simulations using the same paleogeographic and vegetation boundary conditions at a range of atmospheric CO_2 concentrations (Table 1). These new simulations showed more consistent global mean surface temperatures across the ensemble and larger climate sensitivities compared to the EoMIP results[13]. The coordinated experiment set-up allowed a separation of the relative influence of changes in CO_2 concentrations and non-CO_2 boundary conditions (i.e. removal of land ice and prescribed vegetation) on the simulated surface temperatures. Non-CO_2 boundary conditions alone lead to 3-5 °C overall warming and contribute substantially to the reduced meridional temperature gradient, while higher CO_2 levels drive global mean warming due to decreases in atmospheric emissivity. Importantly, three models (CESM1.2-CAM5, GFDL-CM2.1 and NorESM1-F) were able to produce a global surface temperature distribution similar to paleoclimate data at CO_2 concentrations consistent with the geological record.

The DeepMIP-Eocene ensemble has already been used in multiple studies, analysing specific aspects of the Eocene climate in more detail, e.g. the meridional temperature gradient[14], the surface to deep ocean temperature relationship[15], ocean circulation[16], sea ice[17], hydroclimate[18–20], and the impact of mountains[21,22]. We anticipate continued interest in the DeepMIP-Eocene model data, both for model intercomparisons and for model-data syntheses, and aim to document the design of the database and streamline access to improve future re-use of the data. Although the use of large model ensembles is helpful in quantifying the influence of uncertainties in boundary conditions and limitations in model performance on the

simulated Eocene climate, it also presents a technical hurdle in accessing and fully utilising the available data. The use of model-specific data standards, post-processing workflows and variable naming schemes can make the analysis and comparison of multi-model ensembles a tedious process or even lead to processing errors. The need for significant data processing expertise can therefore limit the benefits and wider use of these important data, particularly in non-modelling paleoclimatology disciplines.

Here, we build on the DeepMIP framework to address these issues and present standardised, quality-checked EECO model output to facilitate multi-model processing and analysis, both for model intercomparisons and model-data comparisons. We have reprocessed the output of a total of 26 EECO simulations at CO_2 concentrations between $\times 1$ and $\times 9$ pre-industrial levels, together with their nine pre-industrial reference experiments, to generate a database of common climate variables with consistent temporal averaging, variable names and units across the ensemble. We follow the CMIP convention for variable names and units as closely as possible to take advantage of existing processing workflows, and use the ensemble spread to quantify the internal consistency of the output fields.

We provide two complementary ways of accessing the database, tailored to the most likely future use cases. First, the entire database is stored as global, gridded netCDF (network Common Data Form) files in the Centre for Environmental Data Analysis (CEDA) Archive and can be downloaded as individual files or in batch mode. Combined with the consistent DeepMIP naming convention, this provides a more traditional, scriptable starting point for further analysis. Second, we present an interactive web application to facilitate model-data comparisons of EECO surface temperatures and precipitation. This is a very common use case for paleoclimate model data, but also involves multiple processing steps and potential pitfalls, especially when working with a large model ensemble. The web application automatically calculates paleolocations for a single site or a list of present-day locations, extracts the corresponding model data from the various model grids and plots a summary of the results. The resulting data can be exported for further offline analysis, while the underlying Python code can be used as a starting point for custom analysis.

The database and tools provided are designed to enable data access for non-programmers and to streamline analysis for more advanced users to routinely evaluate existing and emerging paleoclimate data against the full DeepMIP-Eocene model ensemble. This will help to bridge the gap between modelling and data communities to ultimately advance our understanding of early Eocene climate and could potentially serve as a reference framework for similar projects of other geological time periods

in the future.

Methods

DeepMIP-Eocene experiments

All EECO simulations that follow the DeepMIP-Eocene experimental design protocol[12] and are completed by September 2023 form the input data for version 1.0 of the database (Table 1). These simulations are identical to those described in the DeepMIP overview paper[13], with the exception of the new MIROC $\times 1$ and $\times 2$ experiments. The DeepMIP framework provides standardised model boundary conditions and experimental designs to allow a coordinated model intercomparison of the simulation results. All groups have used one of the two reference paleogeographic reconstructions[23,24] interpolated to their respective model grids. Prescribed vegetation and river runoff follow a published reconstruction[23], while globally homogeneous soil parameters based on the global mean of the respective pre-industrial simulation were used. All groups provided a pre-industrial reference simulation and performed a series of EECO experiments, differing only in the concentration of atmospheric CO_2, summarised in Table 2. Other greenhouse gas concentrations and the solar constant were held constant at their pre-industrial levels.

A complete overview of the modelling framework is given in the DeepMIP experimental design paper[12], and detailed descriptions of its implementation in the individual models can be found in the analysis of the large-scale climatic features[13]. We also provide a full description of each model setup based on their published method sections[13] as a README file in the database itself. This is intended to make the downloaded files self-describing and to allow dynamic addition of new experiments and models in the future. In the following, for each model included in version 1.0 of the database, we provide a brief summary of the initialisation and spin-up strategies, as this step required individual decisions by each modelling group. If applicable, we also point out any other deviations from the DeepMIP protocol above.

CESM

Ocean temperatures and salinities in all Eocene simulations are initialised from the same Palaeocene–Eocene Thermal Maximum (PETM; $\sim$55 million years ago) experiment using a previous version of CESM[25,26]. The $\times 1$ simulation was integrated for a further 2600 years, while all other experiments were run for 2000 years.

COSMOS

The $\times 3$ integration was initialised with a homogeneous temperature and salinity of 10 °C and 34.7 psu, respectively, and integrated for an initial 1000 years, after which the $\times 1$ and $\times 4$ simulations were branched. After an initial 8000 years with transient orbital parameters, a constant, pre-industrial orbital configuration was used for the final 1500 years of all simulations. Instead of using the proposed river routing scheme[23], the simulations use a hydrological discharge model that follows the model orography[27].

GFDL

The $\times 1$, $\times 2$, $\times 3$, and $\times 4$ simulations were started from an idealized ocean temperature profile and a globally homogeneous salinity of 34.7 psu. After 1500 and 2000 years of integration, an acceleration technique was applied. Specifically, the linear temperature trends of the last 100 years for each model level below 500 m calculated and the temperature then extrapolated by a 1000 years following this trend. After the second application of this technique at year 2000, the model was run out normally for a further 4000 years for a total of 6000 years. The $\times 6$ simulation was initialised with a globally uniform temperature of 19.32 °C and continously integrated for 6000 years.

HadCM3

Initial ocean temperatures for HadCM3BL were derived from an idealised temperature profile with lowered, CO_2 dependent deep ocean temperatures based on previous Eocene simulations. HadCM3B experiments were branched from the respective HadCM3BL simulations after 4400 to 4900 years and integrated for a further 2950 years. Multiple ocean gateways in the original paleogeography were widened to allow unrestricted ocean circulation and to guarantee the same gateway widths on both the low and high-resolution ocean grids of HadCM3BL and HadCM3B, respectively. In addition, maximum water depths in parts of the Arctic Ocean were reduced to improve numerical stability.

INMCM

The ocean temperature and salinity in the $\times 6$ simulation follow the idealised equations of the DeepMIP protocol[12], but with equatorial surface temperatures lowered by 5 °C. The simulation was integrated for a total of 1150 years.

IPSL

A modified version of the idealised DeepMIP temperature and salinity equations[12], but with overall reduced temperatures, was used to initialise the $\times 3$ simulation. The $\times 1.5$ simulation is branched from the $\times 3$ experiment after 1500 years. Both simulations are run for a total of 4000 years. The ocean bathymetry around individual ocean straits has been manually adjusted

to guarantee the minimum gateway width necessary to allow throughflow.

MIROC

All three simulations have been initialised with a modified version of the idealised DeepMIP temperature and salinity equations[12], with ocean temperatures globally reduced by 15 °C, and integrated for 5000 model years. The $\times 1$ and $\times 2$ experiments are new and have not been included in the DeepMIP overview paper[13].

NorESM

Initial ocean temperatures for the $\times 2$ simulation were used from a previous NorESM-L simulation[28], while salinities were set to 25.5 psu in the Arctic and 34.5 elsewhere. The $\times 4$ simulation was branched off after 100 model years, and both simulations have been run for a further 2000 years. The NorESM simulations were performed with a different paleogeographic reconstruction than the rest of the DeepMIP ensemble (Table 1).

Data processing

We use the raw output of the last 100 years of each of the 35 model simulations as input for our post-processing. For each variable, we generate up to three netCDF output files to facilitate common analysis workflows. We always produce a `mean` file representing either the monthly mean climatology or the annual mean averaged over the last 100 model years, depending on the temporal resolution of the model output. In case of monthly mean output data, the `std` file contains the standard deviation over the same averaging period for each month of the year and can be used for significance testing. Where feasible, we also store the full monthly mean output of the last 100 model years as a `time_series` file to investigate temporal trends or interannual variabilty.

Alongside this standard output, we provide a generic script to interpolate model fields from their native grids to a common resolution for model intercomparisons. The processing workflow requires a local installation of the Climate Data Operator (CDO) software[29] for bilinear or nearest-neighbour interpolation for atmosphere and ocean variables, respectively. Example output for commonly used variables (i.e., near-surface air temperature, sea surface temperature and total precipitation) on a common $1°\times 1°$grid is included in the database and can be directly used for analysis or to verify results of any local postprocessing. The processing script is distributed as part the database (see Data Records section).

Naming convention

We employ a consistent naming convention for variables, directories, and file names across all models to simplify the comparison of different models and to allow a scripted analysis of the entire database. The list of output variables is an extended version of those proposed in the DeepMIP experimental design[12] and is shown in Tables 3-4. Variable names, units and signs of fluxes follow the naming convention of the Coupled Model Intercomparison Project 6 (CMIP6) data request (https://wcrp-cmip.github.io/WGCM_Infrastructure_Panel/CMIP6/data_request.html, last access: 18 October 2023). Consistent standard names, long names and global attributes are directly added to the netCDF files following the Climate and Forecast metadata conventions (CF[30]) in version 1.8 (http://cfconventions.org, last access: 18 October 2023). All netCDF file have been automatically tested for CF-compliance with the `cf-checker` utility (https://github.com/cedadev/cf-checker, last access: 18 October 2023) developed by the UK Met Office and the NCAS Computational Modelling Services (NCAS-CMS). Following the CMIP and CF community standards will both increase user familiarity with the new database and will allow the integration into existing analysis workflows and software. Each output variable is stored in a separate file according to the following structure:

`directory = deepmip-eocene-p1/<Family>/<Model>/<Experiment>/<Version>/<Averaging>/`

`filename = <Variable>_<Model>_<Experiment>_<Version>.<Statistic>.nc`

where:

- `<Family>`, `<Model>` and `<Experiment>` are listed in Table 1 and Table 2, respectively
- `<Variable>` represents the first column in Tables 3-4
- `<Statistic>` is either `mean` (1 or 12 timsteps), `std` (12 timsteps), `time_series` (1200 timsteps) or omitted for the time-independent boundary conditions
- the smaller `mean` and `std` files are stored in the `<Averaging>=climatology` directory and are separated from the larger `time_series` files in the `<Averaging>=time_series` directory to enable more granular download options

Storing all relevant information in the file name itself also allows new phases of coordinated DeepMIP simulations to be integrated into a single database in the future. All output files will be uploaded to the CEDA Archive for long-term storage

after any potential changes arising from the peer-review process have been implemented. During peer-review, all files can be anonymously accessed via Google Drive.

Web application

In addition to depositing the database to the central CEDA repository, we also provide access to a subset of data through a new web application available at https://data.deepmip.org. The website is designed to extract surface temperature and precipitation for any user-defined location from all available model simulations and either visualise the results or download them for offline use. All processing code is written in Python and bundled into a web application via the Streamlit library (https://streamlit.io; last access: 29 September 2023). The code makes full use of the naming conventions described above and is therefore general enough to serve as a template for further in-depth analysis. Detailed instructions on how the application and underlying code can be used to extract subsets from the database are given in the Usage Notes section.

Data Records

The database will be deposited in the CEDA Archive, the UK national data centre for atmospheric and earth observation research, and is currently available via Google Drive. This dataset contains the following types of files:

- **model data:** The directory `deepmip-eocene-p1` contains all processed model output in CF compliant netCDF format[31], a self-describing community standard for storing gridded simulation data, with a total file size of 175.8 GB. Directory and file structure follow the DeepMIP naming convention described above.

- **model READMEs:** Each `<Family>` top-level directory contains a single `<Family>\_README.md` file that contains detailed information about the model, the simulation setup, and output variables available in the respective subdirectories. This ensures the downloaded database is sufficiently self-described and allows the addition of new models and simulation results in the future. The Markdown files are also converted to the PDF format for convenience.

- **validation_tables directory:** PDF files with tables of available output variables for each model, grouped by atmosphere and ocean variables and the respective DeepMIP experiments. The tables also include global minimum/mean/maximum values of all fields for a first-order quality check (see Technical Validation section for details).

- **scripts directory:** Collection of code to interpolate model data to a common grid (`regrid_database_v1.0.sh`), create validation tables of available data (`plot_z-scores_v1.0.py`) and Python dictionaries containing available DeepMIP models, experiments and variables to support scripted analysis of the database (`deepmip_dicts_v1.0.py`).

Technical Validation

An earlier version of the database has already been used in a number of publications[13–15,17–22] to assess the scientific validity of the model simulations, both in terms of model-model and model-data comparisons. In this section, we verify the internal consistency of the database, ensuring that the naming convention has been applied correctly and that the resulting variable names, units and fluxes are consistent across all models. To do this, we automatically parse all `mean` and `time_series` files in the database for any given experiment, interpolate them to a common grid, calculate the global mean, minimum and maximum values and compare these values across all models. We use annual mean fields for the validation of `mean` files and the last 12 available months of the `time_series` files. For variables with multiple vertical levels (see Tables 3-4), we select the vertical index nearest to the 500 hPa pressure level or 1000 m depth for atmospheric and ocean data, respectively. Example tables for atmospheric and ocean `mean` variables from the $\times 3$ simulations are shown in Fig. 1 and Fig. 2, tables for all other experiments as well as for `time_series` files are uploaded to the online database and web application. This testing procedure simulates a standard analysis workflow and is able to detect any deviations from the expected DeepMIP naming convention, while the resulting tables provide a visual overview of available model fields for each experiment. We further calculate the median and standard deviation for each variable and metric across all available models (i.e. for each row in the table) to flag potential outliers that may arise due to inconsistent units or different directions of energy or mass fluxes. For this, we calculate a z-score for each model, variable and statistic which quantifies the number of standard deviations an individual model statistic is above or below the ensemble median. We use the ensemble median instead of the mean as the reference point to reduce the influence of potential outliers in our small sample sizes and calculate the adjusted z-scores as:

$$z = \frac{x - M}{\sigma} \tag{1}$$

where z is the computed z-score, x is the individual model value, M is the median across all available models for the respective variable and statistic (i.e., across each table row), and σ is the standard deviation across the ensemble. A z-score > 3 is commonly used as a cut-off to identify outliers in a distribution. Due to the small sample sizes ($N \leq 9$) the z-score threshold was not used to exclude any data from the database, but rather to find and resolve inconsistencies in the data processing between the models. In the final database, all model fields are within $\pm$ 3 standard deviations around the respective ensemble median, although we note that the small sample sizes allow only an indicative analysis. The Python processing code is included in the online database (see Data Records section) and can be used to develop a custom analysis workflow or to validate any regridding

and global averaging performed by the user.

Usage Notes

We present two primary routes to access the database, either via downloading the netCDF files for local processing or via an interactive website for online model-data comparisons.

netCDF repository

First, processed netCDF files for all simulations will be available from the CEDA Archive. The full directory structure can be accessed via the browser and files can be downloaded via HTTP, Wget, FTP or OPeNDAP. This allows easy access to the data via the browser, as well as scriptable interfaces for bulk downloading. The OPeNDAP (Open-source Project for a Network Data Access Protocol) protocol allows the remote subsetting and exploration of datasets directly in Python, R, IDL, and Matlab. THE CEDA Archive website (https://help.ceda.ac.uk/article/99-download-data-from-ceda-archives; last access: 29 September 2023) gives an up to date overview of all available access options.

Interactive web application

Second, simulated surface temperatures and precipitation from any location can be extracted, visualised and downloaded at https://data.deepmip.org. This allows model-data comparisons via a simple user interface without the need to download the netCDF files locally. The sidebar of the web application can be used to choose between three different analysis pages:

1. **Extract local model data:** Finds the model data closest to a user-specified site (see example in Fig. 3). The minimum inputs are the modern location of the site and the variable of interest (either near-surface air temperature, sea surface temperature, or total precipitation). The application will automatically reconstruct the site's EECO paleo-position on both the mantle[23] and paleomagnetic[24] reference frames and extract the respective monthly and annual mean simulation data from the closest grid point for all models in the database. Model data is interpolated to a common $1° \times 1°$grid (see Data processing section for details) prior to the data selection to eliminate the influence of different model resolutions on the results. In the end, the ensemble means for each experiment are calculated and the results are listed in an interactive table. Data can be downloaded in CSV, Excel or JSON format for direct import into spreadsheets for further offline analysis. The extraction can be performed for a single site or a list of locations and all sites from the DeepMIP proxy database[2] are pre-loaded and available for comparison with the simulation results. Furthermore, the underlying Python functions

`get_paleo_locations()` and `get_model_point_data()` are available in the `deepmip_modules.py` file of the application repository for reuse in any custom analysis. The `get_paleo_locations()` function uses the paleolocation lookup fields provided in the experimental design paper[12] to find the respective early Eocene locations for a list of modern latitude/longitude pairs, using both the mantle[23] and paleomagnetic[24] reference frames. Results are saved in a Pandas DataFrame which can be directly passed to `get_model_point_data()` to extract the nearest model data for all reconstructed locations.

2. **Plot local model data:** Visualises the extracted results and optionally compares them to proxy reconstructions (see example in Fig. 4). Available visualisations include line plots of the annual cycle at the user-specified location, grouped by the various DeepMIP CO_2 levels (Fig. 4a), and a scatter plot of all simulated annual mean values against the respective GMSTs or CO_2 concentrations of the model simulations. (Fig. 4b). The latter plot type can be useful to compare the sensitivity of the model results at the local site against global climate signals. The simulated monthly and annual mean model results can be visually compared against a local proxy reconstruction, either by manually specifying the mean and standard deviation of the proxy data or by loading the respective values for locations from the DeepMIP proxy database[2]. The user can zoom and pan within the interactive figures and download them in PNG and SVG format.

3. **Map sites and boundary conditions:** Plots paleogeographic maps of the chosen site. The user can choose between a global map indicating the location of the study site or regional maps of the bathymetry, orography and land-sea mask on the various native model grids (Fig. 5). The latter can help with the interpretation of the model-data comparison result, e.g. by visualising local grid resolutions and associated intermodel differences in the representation of mountain ranges or ocean gateways.

How to cite the database

This Data Descriptor paper should be cited whenever any netCDF files from the database or results from the web application are reused in a publication. In addition, the user might want to cite the previously published overview of simulated large-scale climate features[13] or the DeepMIP-Eocene experimental design[12], as appropriate.

Code availability

Processing code to interpolate model fields and to create the validation overview tables is included in the online database, currently available via Google Drive. The code for the web application is available at https://github.com/sebsteinig/deepmip-

eocene-app.

References

1. Tierney, J. E. *et al.* Past climates inform our future. *Science* **370**, eaay3701, 10.1126/science.aay3701 (2020).

2. Hollis, C. J. *et al.* The DeepMIP contribution to PMIP4: methodologies for selection, compilation and analysis of latest Paleocene and early Eocene climate proxy data, incorporating version 0.1 of the DeepMIP database. *Geosci. Model. Dev.* **12**, 3149–3206, 10.5194/gmd-12-3149-2019 (2019). Publisher: Copernicus GmbH.

3. Burke, K. D. *et al.* Pliocene and Eocene provide best analogs for near-future climates. *Proc. Natl. Acad. Sci.* **115**, 13288–13293, 10.1073/pnas.1809600115 (2018).

4. Rae, J. W. *et al.* Atmospheric CO_2 over the Past 66 Million Years from Marine Archives. *Annu. Rev. Earth Planet. Sci.* **49**, 609–641, 10.1146/annurev-earth-082420-063026 (2021).

5. Inglis, G. N. *et al.* Global mean surface temperature and climate sensitivity of the early Eocene Climatic Optimum (EECO), Paleocene–Eocene Thermal Maximum (PETM), and latest Paleocene. *Clim. Past* **16**, 1953–1968, 10.5194/cp-16-1953-2020 (2020).

6. Heinemann, M., Jungclaus, J. H. & Marotzke, J. Warm Paleocene/Eocene climate as simulated in ECHAM5/MPI-OM. *Clim. Past* **5**, 785–802, 10.5194/cp-5-785-2009 (2009).

7. Roberts, C. D., LeGrande, A. N. & Tripati, A. K. Climate sensitivity to Arctic seaway restriction during the early Paleogene. *Earth Planet. Sci. Lett.* **286**, 576–585, 10.1016/j.epsl.2009.07.026 (2009).

8. Winguth, A., Shellito, C., Shields, C. & Winguth, C. Climate Response at the Paleocene–Eocene Thermal Maximum to Greenhouse Gas Forcing—A Model Study with CCSM3. *J. Clim.* **23**, 2562–2584, 10.1175/2009JCLI3113.1 (2010).

9. Lunt, D. J. *et al.* CO2-driven ocean circulation changes as an amplifier of Paleocene-Eocene thermal maximum hydrate destabilization. *Geology* **38**, 875–878, 10.1130/G31184.1 (2010).

10. Huber, M. & Caballero, R. The early Eocene equable climate problem revisited. *Clim. Past* **7**, 603–633, 10.5194/cp-7-603-2011 (2011).

11. Lunt, D. J. *et al.* A model-data comparison for a multi-model ensemble of early Eocene atmosphere-ocean simulations: EoMIP. *Clim. Past* **8**, 1717–1736, 10.5194/cp-8-1717-2012 (2012). ISBN: 1814-9340.

12. Lunt, D. J. *et al.* The DeepMIP contribution to PMIP4: experimental design for model simulations of the EECO, PETM, and pre-PETM (version 1.0). *Geosci. Model. Dev.* **10**, 889–901, 10.5194/gmd-10-889-2017 (2017).

13. Lunt, D. J. *et al.* DeepMIP: model intercomparison of early Eocene climatic optimum (EECO) large-scale climate features and comparison with proxy data. *Clim. Past* **17**, 203–227, 10.5194/cp-17-203-2021 (2021).

14. Kelemen, F. D. *et al.* Meridional Heat Transport in the DeepMIP Eocene Ensemble: Non-CO_2 and CO_2 Effects. *Paleoceanogr. Paleoclimatology* **38**, e2022PA004607, 10.1029/2022PA004607 (2023).

15. Goudsmit-Harzevoort, B. *et al.* The Relationship Between the Global Mean Deep-Sea and Surface Temperature During the Early Eocene. *Paleoceanogr. Paleoclimatology* **38**, e2022PA004532, 10.1029/2022PA004532 (2023).

16. Zhang, Y. *et al.* Early Eocene Ocean Meridional Overturning Circulation: The Roles of Atmospheric Forcing and Strait Geometry. *Paleoceanogr. Paleoclimatology* **37**, 10.1029/2021PA004329 (2022). _eprint: https://onlinelibrary.wiley.com/doi/pdf/10.1029/2021PA004329.

17. Niezgodzki, I. *et al.* Simulation of Arctic sea ice within the DeepMIP Eocene ensemble: Thresholds, seasonality and factors controlling sea ice development. *Glob. Planet. Chang.* 103848, 10.1016/j.gloplacha.2022.103848 (2022).

18. Williams, C. J. R. *et al.* African Hydroclimate During the Early Eocene From the DeepMIP Simulations. *Paleoceanogr. Paleoclimatology* **37**, 10.1029/2022PA004419 (2022).

19. Reichgelt, T. *et al.* Plant Proxy Evidence for High Rainfall and Productivity in the Eocene of Australia. *Paleoceanogr. Paleoclimatology* **37**, 10.1029/2022PA004418 (2022).

20. Cramwinckel, M. J. *et al.* Global and Zonal-Mean Hydrological Response to Early Eocene Warmth. *Paleoceanogr. Paleoclimatology* **38**, e2022PA004542, 10.1029/2022PA004542 (2023).

21. Kad, P., Blau, M. T., Ha, K.-J. & Zhu, J. Elevation-dependent temperature response in early Eocene using paleoclimate model experiment. *Environ. Res. Lett.* **17**, 114038, 10.1088/1748-9326/ac9c74 (2022). Publisher: IOP Publishing.

22. Zhang, Z. *et al.* Impact of Mountains in Southern China on the Eocene Climates of East Asia. *J. Geophys. Res. Atmospheres* **127**, 10.1029/2022JD036510 (2022). _eprint: https://onlinelibrary.wiley.com/doi/pdf/10.1029/2022JD036510.

23. Herold, N. *et al.* A suite of early Eocene ($\sim$ 55 Ma) climate model boundary conditions. *Geosci. Model. Dev.* **7**, 2077–2090, 10.5194/gmd-7-2077-2014 (2014).

329 **24.** Baatsen, M. *et al.* Reconstructing geographical boundary conditions for palaeoclimate modelling during the Cenozoic.
330 *Clim. Past* **12**, 1635–1644, 10.5194/cp-12-1635-2016 (2016). Publisher: Copernicus GmbH.

331 **25.** Kiehl, J. T. & Shields, C. A. Sensitivity of the Palaeocene–Eocene Thermal Maximum climate to cloud properties. *Philos.*
332 *Transactions Royal Soc. A: Math. Phys. Eng. Sci.* **371**, 20130093, 10.1098/rsta.2013.0093 (2013). Publisher: Royal Society.

333 **26.** Zhu, J., Poulsen, C. J. & Tierney, J. E. Simulation of Eocene extreme warmth and high climate sensitivity through cloud
334 feedbacks. *Sci. Adv.* 1–11, 10.1126/sciadv.aax1874 (2019).

335 **27.** Hagemann, S. & Dümenil, L. A parametrization of the lateral waterflow for the global scale. *Clim. Dyn.* **14**, 17–31,
336 10.1007/s003820050205 (1998). ISBN: 0930-7575.

337 **28.** Zhang, Z. S. *et al.* Pre-industrial and mid-Pliocene simulations with NorESM-L. *Geosci. Model. Dev.* **5**, 523–533,
338 10.5194/gmd-5-523-2012 (2012).

339 **29.** Schulzweida, U. CDO User Guide, 10.5281/zenodo.7112925 (2022). Publisher: Zenodo Version Number: 2.1.0.

340 **30.** Hassell, D., Gregory, J., Blower, J., Lawrence, B. N. & Taylor, K. E. A data model of the Climate and Forecast
341 metadata conventions (CF-1.6) with a software implementation (cf-python v2.1). *Geosci. Model. Dev.* **10**, 4619–4646,
342 10.5194/gmd-10-4619-2017 (2017).

343 **31.** Rew, R. *et al.* Unidata NetCDF, 10.5065/D6H70CW6 (1989). Language: en Medium: application/java-
344 archive,application/gzip,application/tar.

345 **32.** Zhang, Y. *et al.* Early Eocene vigorous ocean overturning and its contribution to a warm Southern Ocean. *Clim. Past* **16**,
346 1263–1283, 10.5194/cp-16-1263-2020 (2020).

347 Acknowledgements

348 Sebastian Steinig and Daniel J. Lunt acknowledge funding from the NERC SWEET grant (grant no. NE/P01903X/1). Daniel J.
349 Lunt also acknowledges funding from NERC DeepMIP grant (grant no. NE/N006828/1) and the ERC ("The greenhouse earth
350 system" grant; T-GRES, project reference no. 340923, awarded to Rich Pancost). The CESM project is supported primarily by
351 the National Science Foundation (NSF). This material is based upon work supported by the National Center for Atmospheric
352 Research, which is a major facility sponsored by the NSF under Cooperative Agreement No. 1852977. MIROC simulations
353 were supported by funding from KAKENHI grant no. 17H06104 and 17H06323. Gordon. N Inglis was supported by a Royal
354 Society Dorothy Hodgkin Fellowship (DHF\R1\191178) and NERC Large Grant (NE/V018388/1). Agatha de Boer and David

Hutchinson acknowledge support from Swedish Research Council Grant 2016-03912 and FORMAS grant 2018-0162. The GFDL simulations were performed using resources from the Swedish National Infrastructure for Computing (SNIC) at the National Supercomputer Centre (NSC), partially funded by the Swedish Research Council Grant 2018-05973.

Author contributions statement

The model simulations and individual post-processing were carried out by JZ and CJP (CESM), IN and GK (COSMOS), DKH and AMdB (GFDL), SS and DJL (HadCM3), PM and EMV (INMCM), JBL and YD (IPSL), WLC and AAO (MIROC), and ZZ (NorESM). DE, GNI and ANM provided input on the web application and proxy data implementation. SS compiled the final database and developed the web application. SS wrote the manuscript with contributions from all authors.

Competing interests

The authors declare no competing interests relevant to this study.

Figures & Tables

Table 1. Summary of the available DeepMIP-Eocene model simulations in version 1.0 of the database. Experiment short names are defined in Table 2.

Model	Family	PI	×1	×1.5	×2	×3	×4	×6	×9	Geography	Reference
CESM1.2-CAM5	CESM	×	×			×		×	×	[23]	[13, 26]
COSMOS-landveg-r2413	COSMOS	×	×			×	×			[23]	[13]
GFDL-CM2.1	GFDL	×	×		×	×	×	×		[23]	[13]
HadCM3B-M2.1aN	HadCM3	×	×		×	×				[23]	[13]
HadCM3BL-M2.1aN	HadCM3	×	×		×	×				[23]	[13]
INM-CM4-8	INMCM	×						×		[23]	[13]
IPSLCM5A2	IPSL	×		×		×				[23]	[13, 32]
MIROC4m	MIROC	×	×		×	×				[23]	[13]
NorESM1-F	NorESM	×			×		×			[24]	[13]

Table 2. Overview of the DeepMIP-Eocene experiments included in version 1.0 of the database.

Experiment Name	Short Name	CO_2 [ppmv]	Geography
deepmip-eocene-p1-PI	PI	280	modern
deepmip-eocene-p1-x1	x1	280	[23] or [24]
deepmip-eocene-p1-x1.5	x1.5	420	[23] or [24]
deepmip-eocene-p1-x2	x2	560	[23] or [24]
deepmip-eocene-p1-x3	x3	840	[23] or [24]
deepmip-eocene-p1-x4	x4	1120	[23] or [24]
deepmip-eocene-p1-x6	x6	1680	[23] or [24]
deepmip-eocene-p1-x9	x9	2520	[23] or [24]

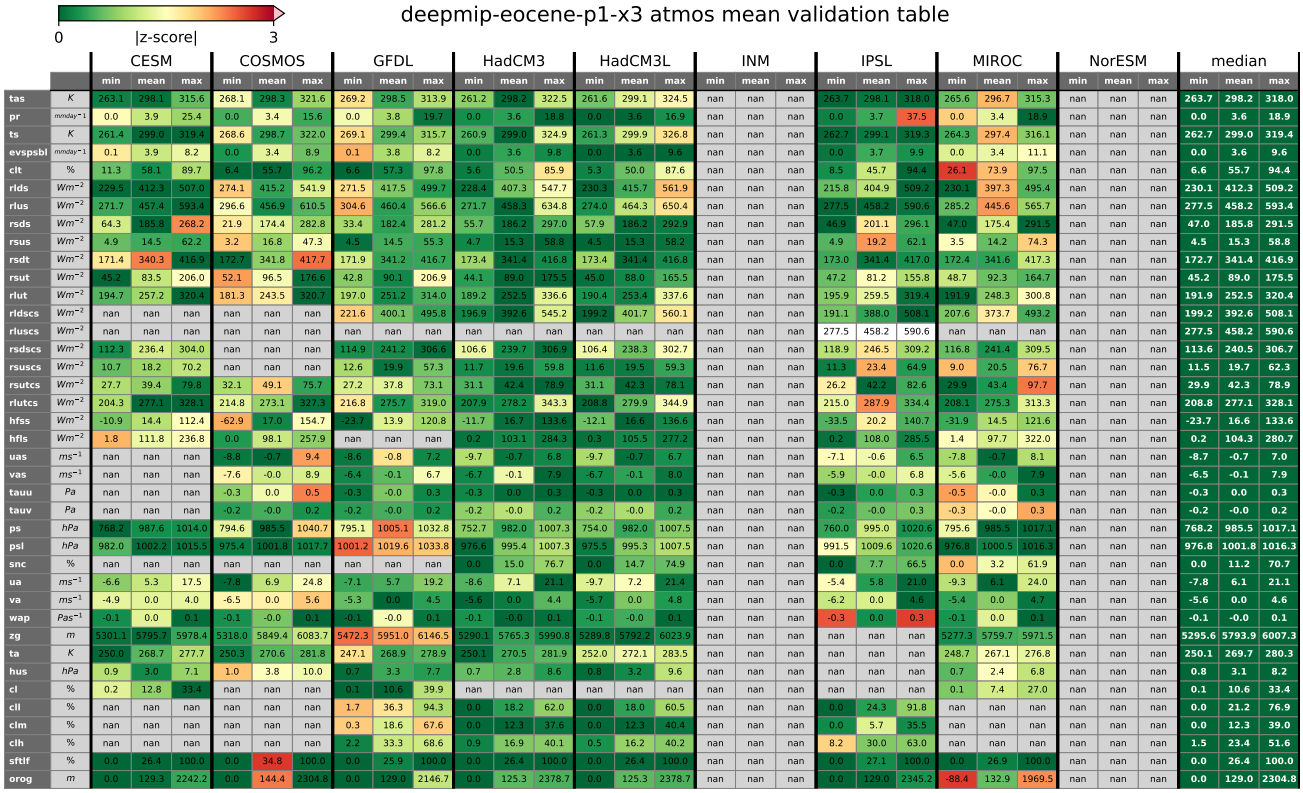

		CESM			COSMOS			GFDL			HadCM3			HadCM3L			INM			IPSL			MIROC			NorESM			median		
		min	mean	max	min	mean	max	min	mean	max	min	mean	max	min	mean	max	min	mean	max	min	mean	max	min	mean	max	min	mean	max	min	mean	max
tas	K	263.1	298.1	315.6	268.1	298.3	321.6	269.2	298.5	313.9	261.2	298.2	322.5	261.6	299.1	324.5	nan	nan	nan	263.7	298.1	318.0	265.6	296.7	315.3	nan	nan	nan	**263.7**	**298.2**	**318.0**
pr	$mm day^{-1}$	0.0	3.9	25.4	0.0	3.4	15.6	0.0	3.8	19.7	0.0	3.6	18.8	0.0	3.6	16.9	nan	nan	nan	0.0	3.7	37.5	0.0	3.4	18.9	nan	nan	nan	**0.0**	**3.6**	**18.9**
ts	K	261.4	299.0	319.4	268.6	298.7	322.0	269.1	299.4	315.7	260.9	299.0	324.9	261.3	299.9	326.8	nan	nan	nan	262.7	299.1	319.3	264.3	297.4	316.1	nan	nan	nan	**262.7**	**299.0**	**319.4**
evspsbl	$mm day^{-1}$	0.1	3.9	8.2	0.0	3.4	8.9	0.1	3.8	8.2	0.0	3.6	9.8	0.0	3.6	9.6	nan	nan	nan	0.0	3.7	9.9	0.0	3.4	11.1	nan	nan	nan	**0.0**	**3.6**	**9.6**
clt	%	11.3	58.1	89.7	6.4	55.7	96.2	6.6	57.3	97.8	5.6	50.5	85.9	5.3	50.0	87.6	nan	nan	nan	8.5	45.7	94.4	26.1	73.9	97.5	nan	nan	nan	**6.6**	**55.7**	**94.4**
rlds	Wm^{-2}	229.5	412.3	507.0	274.1	415.2	541.9	271.5	417.5	499.7	228.4	407.3	547.7	230.3	415.7	561.9	nan	nan	nan	215.8	404.9	509.2	230.1	397.3	495.4	nan	nan	nan	**230.1**	**412.3**	**509.2**
rlus	Wm^{-2}	271.7	457.4	593.4	296.6	456.9	610.5	304.6	460.4	566.6	271.7	458.3	634.8	274.0	464.3	650.4	nan	nan	nan	277.5	458.2	590.6	285.2	445.6	565.7	nan	nan	nan	**277.5**	**458.2**	**593.4**
rsds	Wm^{-2}	64.3	185.8	268.2	21.9	174.4	282.8	33.4	182.4	281.2	55.7	186.2	297.0	57.9	186.2	292.9	nan	nan	nan	46.9	201.1	296.1	47.0	175.4	291.5	nan	nan	nan	**47.0**	**185.8**	**291.5**
rsus	Wm^{-2}	4.9	14.5	62.2	3.2	16.8	47.3	4.5	14.5	55.3	4.7	15.3	58.8	4.5	15.3	58.2	nan	nan	nan	4.9	19.2	62.1	3.5	14.2	74.3	nan	nan	nan	**4.5**	**15.3**	**58.8**
rsdt	Wm^{-2}	171.4	340.3	416.9	172.7	341.8	417.7	171.9	341.2	416.7	173.4	341.4	416.8	173.4	341.4	416.8	nan	nan	nan	173.0	341.4	417.0	172.4	341.6	417.3	nan	nan	nan	**172.7**	**341.4**	**416.9**
rsut	Wm^{-2}	45.2	83.5	206.0	52.1	96.5	176.6	42.8	90.1	206.9	44.1	89.0	175.5	45.0	88.0	165.5	nan	nan	nan	47.2	81.2	155.8	48.7	92.3	164.7	nan	nan	nan	**45.2**	**89.0**	**175.5**
rlut	Wm^{-2}	194.7	257.2	320.4	181.3	243.5	320.7	197.0	251.2	314.0	189.2	252.5	336.6	190.4	253.4	337.6	nan	nan	nan	195.9	259.5	319.4	191.9	248.3	300.8	nan	nan	nan	**191.9**	**252.5**	**320.4**
rldscs	Wm^{-2}	nan	nan	nan	nan	nan	nan	221.6	400.1	495.8	196.9	392.6	545.2	199.2	401.7	560.1	nan	nan	nan	191.1	388.0	508.1	207.6	373.7	493.2	nan	nan	nan	**199.2**	**392.6**	**508.1**
rluscs	Wm^{-2}	nan	nan	nan	nan	nan	nan	nan	nan	nan	nan	nan	nan	nan	nan	nan	nan	nan	nan	277.5	458.2	590.6	nan	nan	nan	nan	nan	nan	**277.5**	**458.2**	**590.6**
rsdscs	Wm^{-2}	112.3	236.4	304.0	nan	nan	nan	114.9	241.2	306.6	106.6	239.7	306.9	106.4	238.3	302.7	nan	nan	nan	118.9	246.5	309.2	116.8	241.4	309.5	nan	nan	nan	**113.6**	**240.5**	**306.7**
rsuscs	Wm^{-2}	10.7	18.2	70.2	nan	nan	nan	12.6	19.9	57.3	11.7	19.6	59.8	11.6	19.5	59.3	nan	nan	nan	11.3	23.4	64.9	9.0	20.5	76.7	nan	nan	nan	**11.5**	**19.7**	**62.3**
rsutcs	Wm^{-2}	27.7	39.4	79.8	32.1	49.1	75.7	27.2	37.8	73.1	31.1	42.4	78.9	31.1	42.3	78.1	nan	nan	nan	26.2	42.2	82.6	29.9	43.4	97.7	nan	nan	nan	**29.9**	**42.3**	**78.9**
rlutcs	Wm^{-2}	204.3	277.1	328.1	214.8	273.1	327.3	216.8	275.7	319.0	207.9	278.2	343.3	208.8	279.9	344.9	nan	nan	nan	215.0	287.9	334.4	208.1	275.3	313.3	nan	nan	nan	**208.8**	**277.1**	**328.1**
hfss	Wm^{-2}	-10.9	14.4	112.4	-62.9	17.0	154.7	-23.7	13.9	120.8	-11.7	16.7	133.6	-12.1	16.6	136.6	nan	nan	nan	-33.5	20.2	140.7	-31.9	14.5	121.6	nan	nan	nan	**-23.7**	**16.6**	**133.6**
hfls	Wm^{-2}	1.8	111.8	236.8	0.0	98.1	257.9	nan	nan	nan	0.2	103.1	284.3	0.3	105.5	277.2	nan	nan	nan	0.2	108.0	285.5	1.4	97.7	322.0	nan	nan	nan	**0.2**	**104.3**	**280.7**
uas	ms^{-1}	nan	nan	nan	-8.8	-0.7	9.4	-8.6	-0.8	7.2	-9.7	-0.7	6.8	-9.7	-0.7	6.7	nan	nan	nan	-7.1	-0.6	6.5	-7.8	-0.7	8.1	nan	nan	nan	**-8.7**	**-0.7**	**7.0**
vas	ms^{-1}	nan	nan	nan	-7.6	-0.0	8.9	-6.4	-0.1	6.7	-6.7	-0.1	7.9	-6.7	-0.1	8.0	nan	nan	nan	-5.9	-0.0	6.8	-5.6	-0.0	7.9	nan	nan	nan	**-6.5**	**-0.1**	**7.9**
tauu	Pa	nan	nan	nan	-0.3	0.0	0.5	-0.3	-0.0	0.3	-0.3	0.0	0.3	-0.3	0.0	0.3	nan	nan	nan	-0.3	0.0	0.3	-0.5	-0.0	0.3	nan	nan	nan	**-0.3**	**0.0**	**0.3**
tauv	Pa	nan	nan	nan	-0.2	-0.0	0.2	-0.2	-0.0	0.2	-0.2	-0.0	0.2	-0.2	-0.0	0.2	nan	nan	nan	-0.2	-0.0	0.3	-0.3	-0.0	0.3	nan	nan	nan	**-0.2**	**-0.0**	**0.2**
ps	hPa	768.2	987.6	1014.0	794.6	985.5	1040.7	795.1	1005.1	1032.8	752.7	982.0	1007.3	754.0	982.0	1007.5	nan	nan	nan	760.0	995.0	1020.6	795.6	985.5	1017.1	nan	nan	nan	**768.2**	**985.5**	**1017.1**
psl	hPa	982.0	1002.2	1015.5	975.4	1001.8	1017.7	1001.2	1019.6	1033.8	976.6	995.4	1007.3	975.5	995.3	1007.5	nan	nan	nan	991.5	1009.6	1020.6	976.8	1000.5	1016.3	nan	nan	nan	**976.8**	**1001.8**	**1016.3**
snc	%	nan	nan	nan	nan	nan	nan	nan	nan	nan	0.0	15.0	76.7	0.0	14.7	74.9	nan	nan	nan	0.0	7.7	66.5	0.0	3.2	61.9	nan	nan	nan	**0.0**	**11.2**	**70.7**
ua	ms^{-1}	-6.6	5.3	17.5	-7.8	6.9	24.8	-7.1	5.7	19.2	-8.6	7.1	21.1	-9.7	7.2	21.4	nan	nan	nan	-5.4	5.8	21.0	-9.3	6.1	24.0	nan	nan	nan	**-7.8**	**6.1**	**21.1**
va	ms^{-1}	-4.9	0.0	4.0	-6.5	0.0	5.6	-5.3	0.0	4.5	-5.6	0.0	4.4	-5.7	0.0	4.8	nan	nan	nan	-6.2	0.0	4.6	-5.4	0.0	4.7	nan	nan	nan	**-5.6**	**0.0**	**4.6**
wap	Pas^{-1}	-0.1	0.0	0.1	-0.1	-0.0	0.1	-0.1	-0.0	0.1	-0.1	-0.0	0.1	-0.1	-0.0	0.1	nan	nan	nan	-0.3	0.0	0.3	-0.1	0.0	0.1	nan	nan	nan	**-0.1**	**-0.0**	**0.1**
zg	m	5301.1	5795.7	5978.4	5318.0	5849.4	6083.7	5472.3	5951.0	6146.5	5290.1	5765.3	5990.8	5289.8	5792.2	6023.9	nan	nan	nan	nan	nan	nan	5277.3	5759.7	5971.5	nan	nan	nan	**5295.6**	**5793.9**	**6007.3**
ta	K	250.0	268.7	277.7	250.3	270.6	281.8	247.1	268.9	278.9	250.1	270.5	281.9	252.0	272.1	283.5	nan	nan	nan	nan	nan	nan	248.7	267.1	276.8	nan	nan	nan	**250.1**	**269.7**	**280.3**
hus	hPa	0.9	3.0	7.1	1.0	3.8	10.0	0.7	3.3	7.7	0.7	2.8	8.6	0.8	3.2	9.6	nan	nan	nan	nan	nan	nan	0.7	2.4	6.8	nan	nan	nan	**0.8**	**3.1**	**8.2**
cl	%	0.2	12.8	33.4	nan	nan	nan	0.1	10.6	39.9	nan	nan	nan	nan	nan	nan	nan	nan	nan	nan	nan	nan	0.1	7.4	27.0	nan	nan	nan	**0.1**	**10.6**	**33.4**
cll	%	nan	nan	nan	nan	nan	nan	1.7	36.3	94.3	0.0	18.2	62.0	0.0	18.0	60.5	nan	nan	nan	0.0	24.3	91.8	nan	nan	nan	nan	nan	nan	**0.0**	**21.2**	**76.9**
clm	%	nan	nan	nan	nan	nan	nan	0.3	18.6	67.6	0.0	12.3	37.6	0.0	12.3	40.4	nan	nan	nan	0.0	5.7	35.5	nan	nan	nan	nan	nan	nan	**0.0**	**12.3**	**39.0**
clh	%	nan	nan	nan	nan	nan	nan	2.2	33.3	68.6	0.9	16.9	40.1	0.5	16.2	40.2	nan	nan	nan	8.2	30.0	63.0	nan	nan	nan	nan	nan	nan	**1.5**	**23.4**	**51.6**
sftlf	%	0.0	26.4	100.0	0.0	34.8	100.0	0.0	25.9	100.0	0.0	26.4	100.0	0.0	26.4	100.0	nan	nan	nan	0.0	27.1	100.0	0.0	26.9	100.0	nan	nan	nan	**0.0**	**26.4**	**100.0**
orog	m	0.0	129.3	2242.2	0.0	144.4	2304.8	0.0	129.0	2146.7	0.0	125.3	2378.7	0.0	125.3	2378.7	nan	nan	nan	0.0	129.0	2345.2	-88.4	132.9	1969.5	nan	nan	nan	**0.0**	**129.0**	**2304.8**

Figure 1. Technical validation of atmospheric global model fields of the $\times 3$ experiment across the ensemble. Variables with multiple vertical levels are shown for the respective model pressure level closest to 500 hPa. Tables for other experiments and "time_series" files can be found in the online database and the web application at https://data.deepmip.org/Validation_tables.

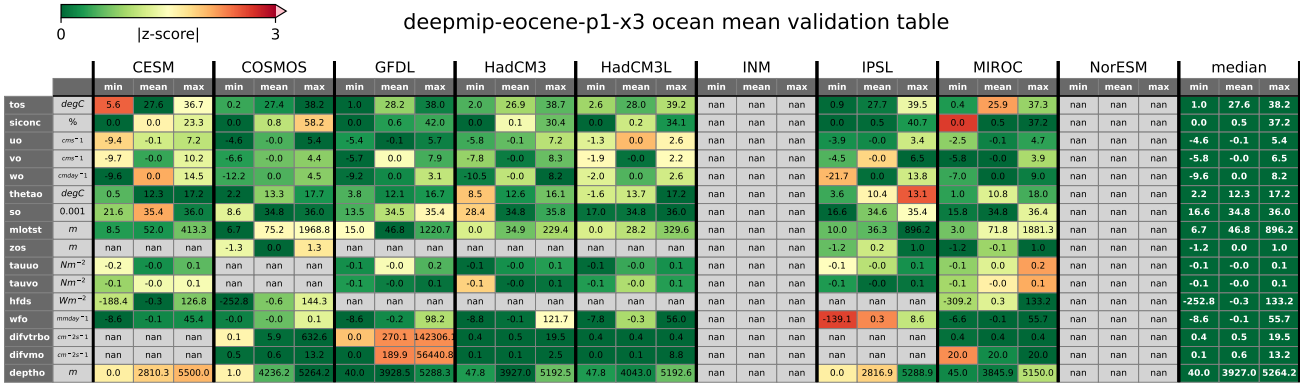

		CESM			COSMOS			GFDL			HadCM3			HadCM3L			INM			IPSL			MIROC			NorESM			median		
		min	mean	max	min	mean	max	min	mean	max	min	mean	max	min	mean	max	min	mean	max	min	mean	max	min	mean	max	min	mean	max	min	mean	max
tos	degC	5.6	27.6	36.7	0.2	27.4	38.2	1.0	28.2	38.0	2.0	26.9	38.7	2.6	28.0	39.2	nan	nan	nan	0.9	27.7	39.5	0.4	25.9	37.3	nan	nan	nan	**1.0**	**27.6**	**38.2**
siconc	%	0.0	0.0	23.3	0.0	0.8	58.2	0.0	0.6	42.0	0.0	0.1	30.4	0.0	0.2	34.1	nan	nan	nan	0.0	0.5	40.7	0.0	0.5	37.2	nan	nan	nan	**0.0**	**0.5**	**37.2**
uo	cms^{-1}	-9.4	-0.1	7.2	-4.6	-0.0	5.4	-5.4	-0.1	5.7	-5.8	-0.1	7.2	-1.3	0.0	2.6	nan	nan	nan	-3.9	-0.0	3.4	-2.5	-0.1	4.7	nan	nan	nan	**-4.6**	**-0.1**	**5.4**
vo	cms^{-1}	-9.7	-0.0	10.2	-6.6	-0.0	4.4	-5.7	0.0	7.9	-7.8	-0.0	8.3	-1.9	-0.0	2.2	nan	nan	nan	-4.5	-0.0	6.5	-5.8	-0.0	3.9	nan	nan	nan	**-5.8**	**-0.0**	**6.5**
wo	$cmday^{-1}$	-9.6	0.0	14.5	-12.2	0.0	4.5	-9.2	0.0	3.1	-10.5	-0.0	8.2	-2.0	0.0	2.6	nan	nan	nan	-21.7	0.0	13.8	-7.0	0.0	9.0	nan	nan	nan	**-9.6**	**0.0**	**8.2**
thetao	degC	0.5	12.3	17.2	2.2	13.3	17.7	3.8	12.1	16.7	8.5	12.6	16.1	-1.6	13.7	17.2	nan	nan	nan	3.6	10.4	13.1	1.0	10.8	18.0	nan	nan	nan	**2.2**	**12.3**	**17.2**
so	0.001	21.6	35.4	36.0	8.6	34.8	36.0	13.5	34.5	35.4	28.4	34.8	35.8	17.0	34.8	36.0	nan	nan	nan	16.6	34.6	35.4	15.8	34.8	36.4	nan	nan	nan	**16.6**	**34.8**	**36.0**
mlotst	m	8.5	52.0	413.3	6.7	75.2	1968.8	15.0	46.8	1220.7	0.0	34.9	229.4	0.0	28.2	329.6	nan	nan	nan	10.0	36.3	896.2	3.0	71.8	1881.3	nan	nan	nan	**6.7**	**46.8**	**896.2**
zos	m	nan	nan	nan	-1.3	0.0	1.3	nan	nan	nan	nan	nan	nan	nan	nan	nan	nan	nan	nan	-1.2	0.2	1.0	-1.2	-0.1	1.0	nan	nan	nan	**-1.2**	**0.0**	**1.0**
tauuo	Nm^{-2}	-0.2	-0.0	0.1	nan	nan	nan	-0.1	-0.0	0.2	-0.1	-0.0	0.1	-0.1	-0.0	0.1	nan	nan	nan	-0.1	-0.0	0.1	-0.1	0.0	0.2	nan	nan	nan	**-0.1**	**-0.0**	**0.1**
tauvo	Nm^{-2}	-0.1	-0.0	0.1	nan	nan	nan	-0.1	-0.0	0.1	-0.1	-0.0	0.1	-0.1	-0.0	0.1	nan	nan	nan	-0.1	-0.0	0.1	-0.1	-0.0	0.1	nan	nan	nan	**-0.1**	**-0.0**	**0.1**
hfds	Wm^{-2}	-188.4	-0.3	126.8	-252.8	-0.6	144.3	nan	nan	nan	nan	nan	nan	nan	nan	nan	nan	nan	nan	nan	nan	nan	-309.2	0.3	133.2	nan	nan	nan	**-252.8**	**-0.3**	**133.2**
wfo	$mmday^{-1}$	-8.6	-0.1	45.4	-0.0	-0.0	0.1	-8.6	-0.2	98.2	-8.8	-0.1	121.7	-7.8	-0.3	56.0	nan	nan	nan	-139.1	0.3	8.6	-6.6	-0.1	55.7	nan	nan	nan	**-8.6**	**-0.1**	**55.7**
difvtrbo	cm^2s^{-1}	nan	nan	nan	0.1	5.9	632.6	0.0	270.1	142306.1	0.4	0.5	19.5	0.4	0.4	0.4	nan	nan	nan	nan	nan	nan	0.4	0.4	0.4	nan	nan	nan	**0.4**	**0.5**	**19.5**
difvmo	cm^2s^{-1}	nan	nan	nan	0.5	0.6	13.2	0.0	189.9	56440.8	0.1	0.1	2.5	0.0	0.1	8.8	nan	nan	nan	nan	nan	nan	20.0	20.0	20.0	nan	nan	nan	**0.1**	**0.6**	**13.2**
deptho	m	0.0	2810.3	5500.0	1.0	4236.2	5264.2	40.0	3928.5	5288.3	47.8	3927.0	5192.5	47.8	4043.0	5192.6	nan	nan	nan	0.0	2816.9	5288.9	45.0	3845.9	5150.0	nan	nan	nan	**40.0**	**3927.0**	**5264.2**

Figure 2. Technical validation of ocean global model fields of the $\times 3$ experiment across the ensemble. Variables with multiple vertical levels are shown for the respective model depth closest to 1000 m. Tables for other experiments and "time_series" files can be found in the online database and the web application at https://data.deepmip.org/Validation_tables.

Table 3. Atmosphere output variables included in version 1.0 of the database. Naming conventions follow the CMIP6 data request.

Name	Long Name	Units	Dimensions
tas	Near-Surface Air Temperature	K	time×lat×lon
ts	Surface Temperature	K	time×lat×lon
pr	Precipitation	$kg\ m^{-2}\ s^{-1}$	time×lat×lon
evspsbl	Evaporation Including Sublimation and Transpiration	$kg\ m^{-2}\ s^{-1}$	time×lat×lon
hfls	Surface Upward Latent Heat Flux	$W\ m^{-2}$	time×lat×lon
hfss	Surface Upward Sensible Heat Flux	$W\ m^{-2}$	time×lat×lon
ps	Surface Air Pressure	Pa	time×lat×lon
psl	Sea Level Pressure	Pa	time×lat×lon
snc	Snow Area Fraction	%	time×lat×lon
rsds	Surface Downwelling Shortwave Radiation	$W\ m^{-2}$	time×lat×lon
rlds	Surface Downwelling Longwave Radiation	$W\ m^{-2}$	time×lat×lon
rsus	Surface Upwelling Shortwave Radiation	$W\ m^{-2}$	time×lat×lon
rlus	Surface Upwelling Longwave Radiation	$W\ m^{-2}$	time×lat×lon
rsdt	TOA Incident Shortwave Radiation	$W\ m^{-2}$	time×lat×lon
rsut	TOA Outgoing Shortwave Radiation	$W\ m^{-2}$	time×lat×lon
rlut	TOA Outgoing Longwave Radiation	$W\ m^{-2}$	time×lat×lon
rsdscs	Surface Downwelling Clear-Sky Shortwave Radiation	$W\ m^{-2}$	time×lat×lon
rldscs	Surface Downwelling Clear-Sky Longwave Radiation	$W\ m^{-2}$	time×lat×lon
rsuscs	Surface Upwelling Clear-Sky Shortwave Radiation	$W\ m^{-2}$	time×lat×lon
rluscs	Surface Upwelling Clear-Sky Longwave Radiation	$W\ m^{-2}$	time×lat×lon
rsutcs	TOA Outgoing Clear-Sky Shortwave Radiation	$W\ m^{-2}$	time×lat×lon
rlutcs	TOA Outgoing Clear-Sky Longwave Radiation	$W\ m^{-2}$	time×lat×lon
tauu	Surface Downward Eastward Wind Stress	Pa	time×lat×lon
tauv	Surface Downward Northward Wind Stress	Pa	time×lat×lon
uas	Eastward Near-Surface Wind	$W\ m^{-2}$	time×lat×lon
vas	Northward Near-Surface Wind	$W\ m^{-2}$	time×lat×lon
clh	High Level Cloud Fraction	%	time×lat×lon
clm	Mid Level Cloud Fraction	%	time×lat×lon
cll	Low Level Cloud Fraction	%	time×lat×lon
clt	Total Cloud Cover Percentage	%	time×lat×lon
cl	Percentage Cloud Cover	%	level×time×lat×lon
hus	Specific Humidity	1	level×time×lat×lon
ta	Air Temperature	K	level×time×lat×lon
ua	Eastward Wind	$m\ s^{-1}$	level×time×lat×lon
va	Northward Wind	$m\ s^{-1}$	level×time×lat×lon
wap	Omega (=dp/dt)	$Pa\ s^{-1}$	level×time×lat×lon
zg	Geopotential Height	m	level×time×lat×lon
orog	Surface Altitude	m	lat×lon
sftlf	Percentage of the Grid Cell Occupied by Land	%	lat×lon

Table 4. Ocean output variables included in version 1.0 of the database. Naming conventions follow the CMIP6 data request.

Name	Long Name	Units	Dimensions
tos	Sea Surface Temperature	$°C$	time×lat×lon
siconc	Sea-Ice Area Percentage (Ocean Grid)	$\%$	time×lat×lon
mlotst	Ocean Mixed Layer Thickness Defined by Sigma T	m	time×lat×lon
zos	Sea Surface Height Above Geoid	m	time×lat×lon
hfds	Downward Heat Flux at Sea Water Surface	$W\ m^{-2}$	time×lat×lon
wfo	Water Flux Into Sea Water	$kg\ m^{-2}\ s^{-1}$	time×lat×lon
tauuo	Sea Water Surface Downward X Stress	$N\ m^{-2}$	time×lat×lon
tauvo	Sea Water Surface Downward Y Stress	$N\ m^{-2}$	time×lat×lon
msftbarot	Ocean Barotropic Mass Streamfunction	$kg\ s^{-1}$	time×lat×lon
msftmz	Ocean Meridional Overturning Mass Streamfunction	$kg\ s^{-1}$	time×depth×lat
so	Sea Water Salinity	0.001	depth×time×lat×lon
thetao	Sea Water Potential Temperature	$°C$	depth×time×lat×lon
uo	Sea Water X Velocity	$m\ s^{-1}$	depth×time×lat×lon
vo	Sea Water Y Velocity	$m\ s^{-1}$	depth×time×lat×lon
wo	Sea Water Vertical Velocity	$m\ s^{-1}$	depth×time×lat×lon
difvmo	Ocean Vertical Momentum Diffusivity	$m^{-2}\ s^{-1}$	depth×time×lat×lon
difvtrbo	Ocean Vertical Tracer Diffusivity Due to Background	$m^{-2}\ s^{-1}$	depth×time×lat×lon
deptho	Sea Floor Depth Below Geoid	m	lat×lon

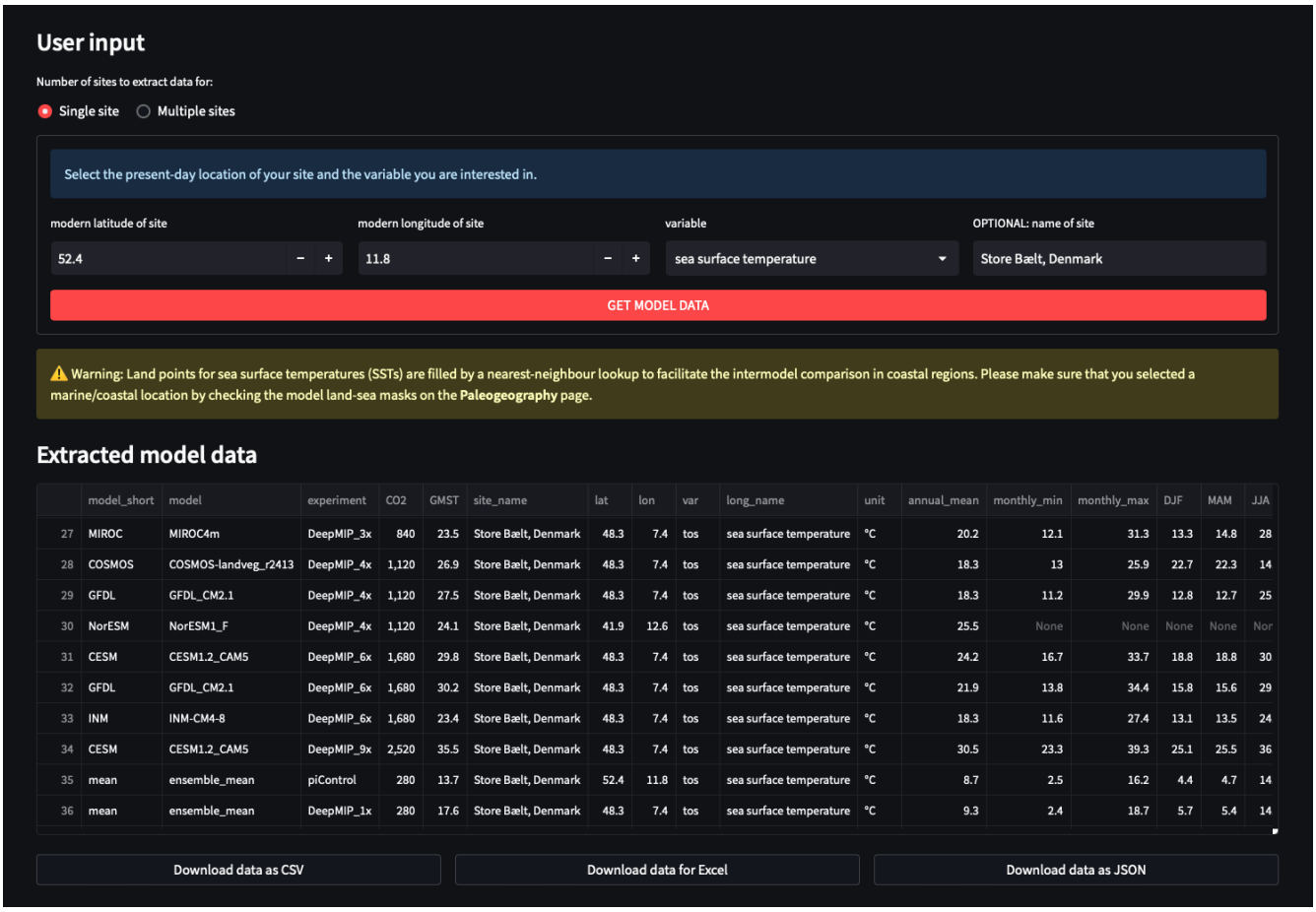

	model_short	model	experiment	CO2	GMST	site_name	lat	lon	var	long_name	unit	annual_mean	monthly_min	monthly_max	DJF	MAM	JJA
27	MIROC	MIROC4m	DeepMIP_3x	840	23.5	Store Bælt, Denmark	48.3	7.4	tos	sea surface temperature	°C	20.2	12.1	31.3	13.3	14.8	28
28	COSMOS	COSMOS-landveg_r2413	DeepMIP_4x	1,120	26.9	Store Bælt, Denmark	48.3	7.4	tos	sea surface temperature	°C	18.3	13	25.9	22.7	22.3	14
29	GFDL	GFDL_CM2.1	DeepMIP_4x	1,120	27.5	Store Bælt, Denmark	48.3	7.4	tos	sea surface temperature	°C	18.3	11.2	29.9	12.8	12.7	25
30	NorESM	NorESM1_F	DeepMIP_4x	1,120	24.1	Store Bælt, Denmark	41.9	12.6	tos	sea surface temperature	°C	25.5	None	None	None	None	Nor
31	CESM	CESM1.2_CAM5	DeepMIP_6x	1,680	29.8	Store Bælt, Denmark	48.3	7.4	tos	sea surface temperature	°C	24.2	16.7	33.7	18.8	18.8	30
32	GFDL	GFDL_CM2.1	DeepMIP_6x	1,680	30.2	Store Bælt, Denmark	48.3	7.4	tos	sea surface temperature	°C	21.9	13.8	34.4	15.8	15.6	29
33	INM	INM-CM4-8	DeepMIP_6x	1,680	23.4	Store Bælt, Denmark	48.3	7.4	tos	sea surface temperature	°C	18.3	11.6	27.4	13.1	13.5	24
34	CESM	CESM1.2_CAM5	DeepMIP_9x	2,520	35.5	Store Bælt, Denmark	48.3	7.4	tos	sea surface temperature	°C	30.5	23.3	39.3	25.1	25.5	36
35	mean	ensemble_mean	piControl	280	13.7	Store Bælt, Denmark	52.4	11.8	tos	sea surface temperature	°C	8.7	2.5	16.2	4.4	4.7	14
36	mean	ensemble_mean	DeepMIP_1x	280	17.6	Store Bælt, Denmark	48.3	7.4	tos	sea surface temperature	°C	9.3	2.4	18.7	5.7	5.4	14

Figure 3. Example user input and extracted model data for a single site in the web application.

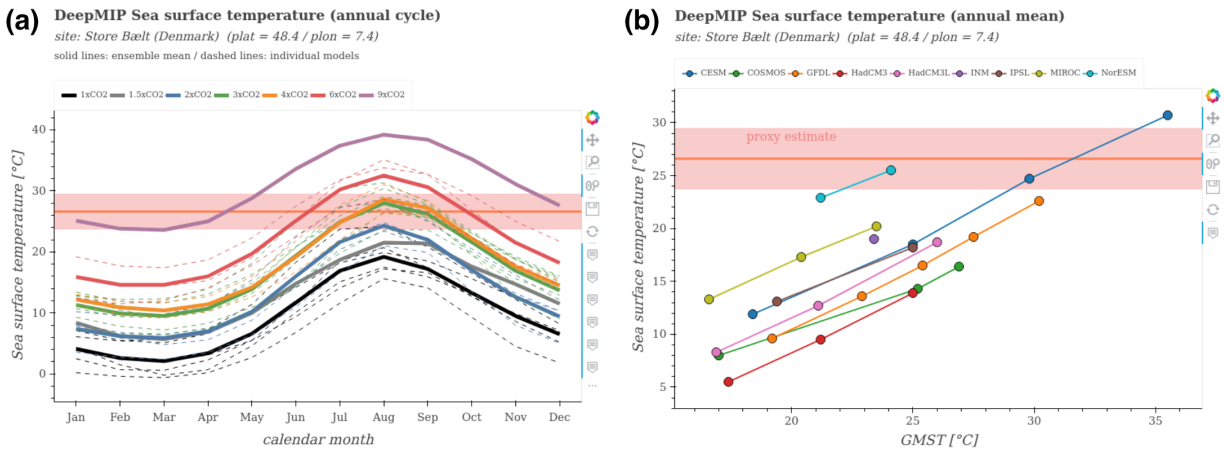

Figure 4. Example graphical output of the web application for the model-data comparison of the Store Bælt (Denmark) site defined in Fig. 3. (a) Simulated annual cycle of sea surface temperatures at the respective grid point closest to the reconstructed paleoposition of the site. Solid lines show the ensemble mean for each CO_2 concentration with individual models represented by the dashed lines. (b) Scatter plot of the simulated annual mean sea surface temperature at the proxy site compared to the global mean surface temperature of the respective simulation. Lines connect results of the same model. Reconstructed proxy temperature is based on the TEX_{86} paleothermometer[2].

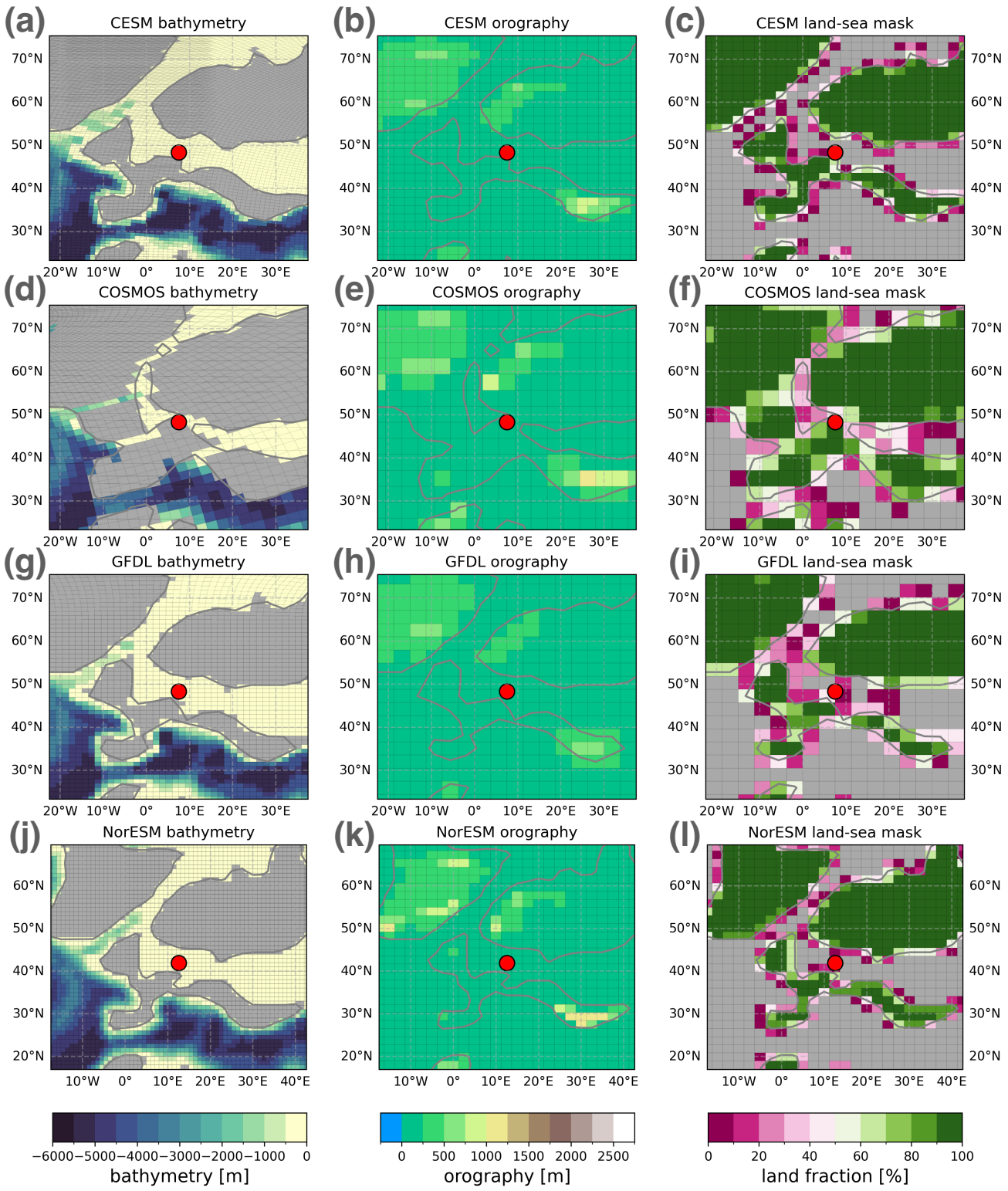

Figure 5. Maps of local boundary condition differences between some of the models around the the Store Bælt (Denmark) site defined in Fig. 3 produced by the web application. The reconstructed paleoposition of the site (red dot) represents a land point in COSMOS (panel d-f) and ocean points in the other models. Note the different paleogeographic reconstruction used in NorESM (panel j-l).